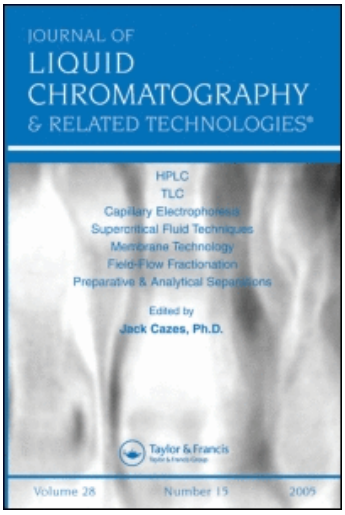

Journal of Liquid Chromatography & Related Technologies
Publication details, including instructions for authors and subscription information:
http://www.informaworld.com/smpp/title~content=t713597273

Analysis of the Mechanism of Retention on a Modified β-Cyclodextrin/Silica Chiral Stationary Phase using a Computational Chemical Method

Fairouz Tazerouti[a]; Ahmed Yacine Badjah-Hadj-Ahmed[a]; Toshihiko Hanai[b]
[a] Faculté de Chimie, Laboratoire d'Analyse Organique Fonctionnelle, U.S.T.H.B., Alger, Algeria [b] Health Research Foundation, Institut Pasteur, Kyoto, Japan

To cite this Article Tazerouti, Fairouz , Badjah-Hadj-Ahmed, Ahmed Yacine and Hanai, Toshihiko(2007) 'Analysis of the Mechanism of Retention on a Modified β-Cyclodextrin/Silica Chiral Stationary Phase using a Computational Chemical Method', Journal of Liquid Chromatography & Related Technologies, 30: 20, 3043 — 3057
To link to this Article: DOI: 10.1080/10826070701632345
URL: http://dx.doi.org/10.1080/10826070701632345

Journal of Liquid Chromatography & Related Technologies®, 30: 3043–3057, 2007

ISSN 1082-6076 print/1520-572X online
DOI: 10.1080/10826070701632345

Analysis of the Mechanism of Retention on a Modified β-Cyclodextrin/Silica Chiral Stationary Phase using a Computational Chemical Method

Fairouz Tazerouti and Ahmed Yacine Badjah-Hadj-Ahmed
Faculté de Chimie, Laboratoire d'Analyse Organique Fonctionnelle, U.S.T.H.B., Alger, Algeria

Toshihiko Hanai
Health Research Foundation, Institut Pasteur, Kyoto, Japan

Abstract: Quantitative analysis of the retention of various optically active solutes on a modified β-cyclodextrin/silica chiral stationary phase was achieved using a molecular mechanics calculation of the CAChe program. Using computational chemical calculations, the various interactions between each enantiomer and the modified β-cyclodextrin chiral selector were calculated as energy contributions. These interaction energy values were then compared to the experimental values measured in normal phase liquid chromatography. Among the obtained predicted values, the best correlation was observed between the molecular interaction energy and the selectivity factor, α, calculated for the studied racemates.

Keywords: Computational chemical analysis, Chiral separation, Modified cyclodextrin, HPLC, Drugs, Herbicides

INTRODUCTION

Computational chemistry using a model phase is a convenient method for evaluating and quantitatively analyzing retention in high performance liquid

Address correspondence to Toshihiko Hanai, Health Research Foundation, Institut Pasteur 5F, Tanaka-Monzencho, Sakyo-ku, Kyoto 606-8225, Japan. E-mail: thanai@attglobal.net

chromatography. This simulation technique allows for an acceptable determination of the various contributions to the interaction between the solute and packing material surfaces. Hydrophobic interactions are related to a change in the van der Waals (VW) energy value, whereas polar interactions are related to either a change in the electrostatic (ES) energy value or hydrogen bonding (HB) energy, which also contributes to this kind of interaction.

In the case of a homologous series like phenolic compounds, the retention mechanisms can be quantitatively analyzed using a simple model phase.[1] In the case of more complex solutes such as drugs, the molecular interaction energy values are easily calculated using a simple model phase, whereas evaluation of VW energy contribution related to the contact surface area between the analyte and the model phase requires a three dimensional model.[2]

On the other hand, computational chemical methods are also useful for evaluating the value of the selectivity of various synthesised chiral stationary phases, particularly Pirkle type phases that involve very few stereocenters.[3–10] The prediction of the elution order of enantiomers is possible, whereas the calculated separation factors do not agree with the experimental values.

Cyclodextrin (CD) and its derivatives are models for studying inclusion mechanisms using computational chemical analysis. The molecular dynamics simulations indicate that tryptophan is localized on the interior of α-CD.[11] The molecular mechanics (MM) and molecular dynamics calculations for a 1:1 complex of binaphthyl derivatives by heptakis (2,3,6-tri-O-methyl)-β-CD suggest that VW contacts and intermolecular hydrogen bonding stabilize the complex,[12] as well as the dipole-dipole interactions between the host and guest.[13] The enantiomers of 1- and 2-naphthylethanols with β-CD are complex structures with different geometries mixed. Stereoselectivity in the rigid 2:2 complexes is more readily observed than in the more flexible 1:1 complexes.[14] The asymmetrical twisted shape of the host cavity seems to be the origin of chiral recognition by CD based on the study of a modified CD-metal complex.[15]

The conformation of 4a*S*/*R*-galanthamine diastereoisomers and α-CD were studied using docking and molecular dynamics simulation approaches. The binding energy of the constructed 4a*R*-galanthamine-α-CD complexes was approximately 17 kcal/mol lower than that of 4a*S*-galanthamine-α-CD, implying that the binding ability of 4a*R*-galanthamine with α-CD is stronger than that of 4a*S*-galanthamine. The hydrophobic interaction between the guest and host is the main binding force for the formation of a stable 4 a*R*-galanthamine-α-CD complex.[16] *S*-Binaphthyl forms a more stable complex with β-CD than the corresponding *R*-enantiomer, as determined by the binding energy difference.[17]

The interaction energies of the dansyl-amino acid with five CDs were calculated. Molecular modeling was not performed to study enantioselectivity, because subtle differences in the interactions between CDs and enantiomer pairs require extremely long, comprehensive modeling approaches.[18,19] The development of computer hard- and software, however, facilitated the study.

Table 1. List of analytes

No	Analytes
1	1,1′-Bi-2-naphthol
2	2,2-Dimethoxy-1,1′-binaphthalene
3	2-Naphthylethanol
4	*trans*-2-Phenyl-3-(4-chlorophenyl)-oxirane
5	*trans*-2,3-Diphenyloxirane
6	*N*-(3,5-Dinitrobenzoyl)-2-aminomethylpropanoate
7	*N*-(3,5-Dinitrobenzoyl)-2-amino-3-methylmethylbutanoate
8	*N*-(3,5-Dinitrobenzoyl)-2-amino-3-phenylmethylpropanoate
9	*N*-(3,5-Dimethylbenzoyl)-2-aminomethylpropanoate
10	9-Anthryl-2,2,2-trifluoroethanol
11	*N*-(3,5-Dinitrobenzoyl)-1-phenylethanamine
12	*O*-(3,5-Dinitrobenzoyl)-1-(2-naphthyl)-ethanol
13	*N*-(3,5-Dinitrobenzoyl)-1-(1-naphthyl)-ethanamine
14	Troger base
15	Butylfluazifop
16	Ethoxyethylhaloxyfop
17	Ethoxyethylchlorazifop
18	Methyldichlofop
19	Propranolol
20	Indapamide
21	Phenoxypropionic acid
22	2-Chlorophenoxypropionic acid
23	3-Chlorophenoxypropionic acid
24	4-Chlorophenoxypropionic acid
25	Dichloprop
26	Silvex
27	Mecoprop
28	Ibuprofen
29	Mandelic acid

In this paper, the inclusion complexes formed between β-CD and various optically active solutes (drugs and herbicides, Table 1) were modeled and refined using molecular modeling methods. The interaction energies of the formed complexes calculated for both enantiomers correlated with the experimental retention data measured in normal mode HPLC.[20]

EXPERIMENTAL

The computer was a Dell model Latitude C840 equipped with a 2-GHz processor and 1024MB of memory. The molecular properties of the analytes, model phases, and molecular interactions were calculated by MM2

from version 5 of the CAChe program from Fujitsu, Tokyo, Japan. The standard parameters used were bond stretch, bond angle, dihedral angle, improper torsion, VW, hydrogen bonding, and electrostatic interactions (MM2/MM3 bond dipoles). The VW cut-off distance was 9 Å. The energy unit was kcal/mole (1 kJ/mol = 4.18 kcal/mol). The molecular design was based on the capacity of the computer used. The optimized energy value was less than 0.00001 kcal/mol.

RESULTS AND DISCUSSION

A model CD containing 441 atoms, 469 bonds, and 3513 connectors was first constructed as a model phase and the molecular interaction energy between this model phase and a standard compound was calculated using MM2 from version 5 of the CAChe program.

In this study, the calculations were performed with the small opening "locked" using phenylcarbamate groups, while the large opening of the CD ring was unlocked, allowing for inclusion of the guest solute. Figure 1 shows an example of the optimised analyte structure (6*R*) and a partly locked derivatized CD complex. A completely unlocked chiral stationary phase, in which the structure is deformed, was not suitable for this approach (Figure 2), and the initial condition before docking affected the final structure. A possible reason for this phenomenon is that the constructed model phase might not be perfect for the quantitative analysis of molecular interactions.

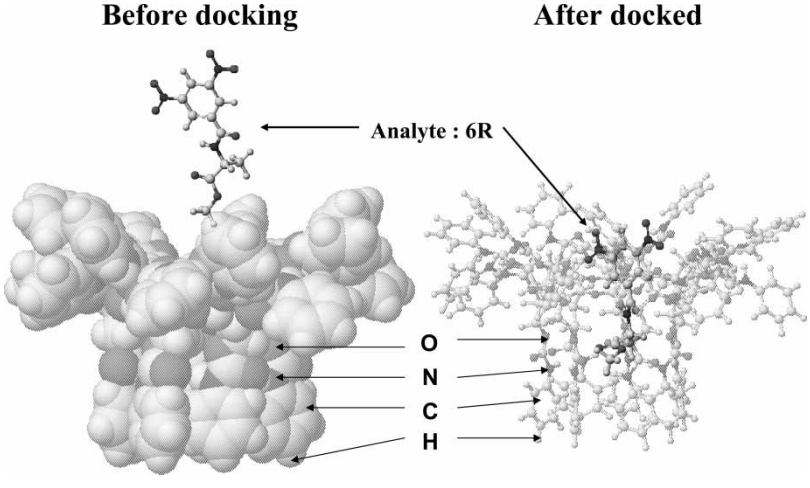

Figure 1. Optimised structure of an analyte (6*R*) and a partly locked derivatized cyclodextrin complex. Small white ball: hydrogen; gray ball: carbon; dark gray ball: nitrogen; black ball: oxygen.

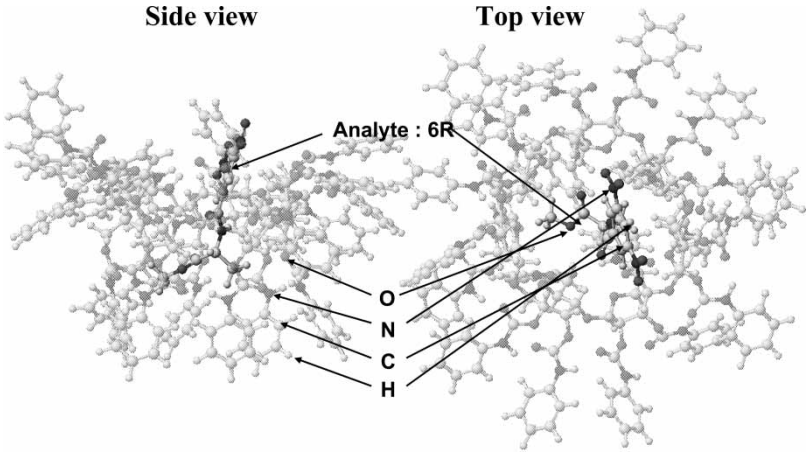

Figure 2. Optimised structure of an analyte (6*R*) and an unlocked derivatized cyclodextrin complex. Small white ball: hydrogen; gray ball: carbon; dark gray ball: nitrogen; black ball: oxygen.

The calculated energy values are summarized in Table 2 where the energy values of single analytes were: fs: final structure; hb: hydrogen bonding; es: electrostatic, and vw: van der Waals while FS: final structure; HB: hydrogen bonding; ES: electrostatic and VW: van der Waals were energy values of the complex, and the molecular interaction energy values were represented by ΔFS, ΔHB, ΔES, and ΔVW. The calculated values were the lowest energy values of each compound and complex. The ΔHB, ΔES, and ΔVW were used to study the contribution to the molecular interaction. As a preliminary study, we compared the different energy values (ΔFS, ΔHB, ΔES, and ΔVW) for each enantiomer couple with its selectivity (α).

A comparison of the calculated interaction energy values with the measured retention factors and selectivities indicated that the best correlation was observed between the final structure interaction energy ΔFS and α selectivity (Table 3). Thus, when the energy term ΔFS is significant, enantioseparation occurs regardless of the values of the other energy parameters ΔHB, ΔES, and ΔVW.

On the other hand, when both enantiomer complexes give close ΔFS values, no resolution is observed in HPLC, even if ΔHB, ΔES, and ΔVW are quite different (e.g., solutes 14 and 16). This correlation explains why we considered the ΔFS parameter to be the most significant molecular interaction energy value. We noticed that the greater the difference between ΔFS, the higher the measured calculated selectivity (α) for most racemates. To evaluate the threshold limit of enantioseparation in terms of ΔFS energy, we correlated the difference Δ(ΔFS) for each couple with its α value (Table 3).

Table 2. Molecular properties of analytes and complexes

No	fs	hb	es	vw	FS	HB	ES	VW
1a	−42.0813	−12.524	−0.073	13.014	−67.8839	−171.808	−432.465	234.555
1b	−43.8243	−14.536	−0.301	13.571	−66.2554	−175.915	−434.109	236.240
2a	−24.3721	0.000	−0.025	10.778	−49.7791	−149.827	−429.851	225.261
2b	−24.3721	0.000	−0.025	10.778	−50.3818	−151.979	−431.146	224.300
3*R*2	−21.1775	−3.012	−0.987	6.693	−52.6655	−166.629	−434.383	223.241
3*S*2	−21.7950	−2.999	−0.997	6.205	−51.8824	−166.013	−434.256	222.861
4*RR*	95.0669	0.000	0.049	4.659	49.3740	−157.455	−430.741	216.306
4*SS*	95.0671	0.000	0.048	4.659	51.2440	−157.095	−430.799	217.666
5*RR*	94.8670	0.000	0.100	4.478	50.9872	−160.609	−432.813	217.433
5*SS*	94.8670	0.000	0.100	4.478	50.5432	−161.174	−432.757	217.441
6*R*	−9.5993	−5.511	−5.765	11.165	−37.7840	−168.238	−436.183	227.332
6*S*	−9.5969	−5.575	−5.763	11.120	−38.2176	−165.290	−439.355	225.183
7*R*	−9.7997	−4.837	−4.873	11.580	−34.1269	−160.034	−439.738	227.202
7*S*	−8.1314	−3.638	−5.712	12.017	−33.2391	−157.968	−437.211	227.234
8*R*	−21.0007	−5.159	−5.998	12.433	−53.2718	−164.958	−436.086	229.831
8*S*	−23.4939	−7.658	−4.948	13.203	−53.2752	−166.940	−436.696	221.244
9*R*	−10.4416	−5.357	−6.379	8.681	−38.3941	−163.862	−439.602	228.029
9*S*	−12.1933	−4.055	−6.236	8.948	−43.1784	−167.485	−443.336	220.553
10*R*	−4.0153	−4.845	21.819	11.971	−19.3381	−160.040	−410.851	235.402
10*S*	−4.0153	−4.844	21.818	11.974	−19.0174	−162.050	−412.504	235.203
11*R*	−32.9582	−5.540	−18.128	11.968	−58.3975	−163.424	−450.274	226.802
11*S*	−32.9061	−5.549	−18.109	11.878	−59.1601	−166.066	−452.227	225.866
12*R*	−43.6639	−5.563	−18.124	14.800	−82.2147	−166.448	−450.842	219.539
12*S*	−43.6674	−5.565	−18.126	14.729	−81.9278	−166.738	−450.738	219.525

13*R*	−38.0657	−4.420	−17.695	15.405	−73.9923	−162.388	−449.135	223.503
13*S*	−38.0786	−4.496	−17.704	15.372	−72.6351	−164.220	−447.299	224.188
14*RR*	18.3445	0.000	−23.696	15.446	−12.3379	−153.248	−455.193	224.052
14*SS*	18.3439	0.000	−23.696	15.445	−15.0529	−158.954	−456.903	221.900
15*R*	−8.4325	0.000	−6.532	8.768	−48.1309	−154.634	−438.562	213.951
15*S*	−8.4299	0.000	−6.533	8.770	−48.0557	−150.586	−437.523	209.890
16*R*	−1.6885	0.000	−1.960	9.998	−46.1194	−159.996	−437.252	210.920
16*S*	−1.6873	0.000	−1.960	9.998	−47.1236	−158.063	−435.012	211.393
17*R*	−0.4602	0.000	3.639	9.782	−40.9189	−149.936	−426.481	212.747
17*S*	−0.4599	0.000	3.638	9.784	−40.6286	−158.640	−431.986	211.664
18*R*	−13.7266	0.000	−2.134	7.301	−52.2646	−154.807	−433.845	215.776
18*S*	−13.7258	0.000	−2.135	7.302	−52.2357	−154.793	−433.834	215.040
19*R*	0.3921	−6.153	4.408	9.868	−26.7313	−165.027	−429.185	219.503
19*S*	0.3926	−6.152	4.407	9.880	−27.9734	−162.104	−427.098	220.028
20*R*	−8.4366	−1.874	2.774	10.201	−38.1711	−155.185	−429.171	221.843
20*S*	−9.2404	−2.113	2.157	10.265	−38.3116	−155.185	−429.345	221.682
21*R*	1.8345	−18.016	21.985	4.374	−37.2694	−179.195	−410.682	220.682
21*S*	1.8346	−18.015	21.985	4.374	−38.6503	−182.152	−408.606	219.368
22*R*	3.4301	−18.006	23.328	4.587	−36.3664	−183.933	−413.599	215.675
22*S*	3.4299	−18.019	23.336	4.592	−38.4050	−187.107	−412.443	218.074
23*R*	2.1194	−18.005	22.015	4.547	−38.3160	−193.905	−412.628	222.828
23*S*	2.1192	−18.015	22.020	4.550	−40.5067	−189.368	−414.082	218.791
24*R*	2.1132	−18.042	22.030	4.551	−39.8812	−181.655	−410.690	219.385
24*S*	2.1174	−17.996	22.001	4.533	−42.3698	−185.755	−413.370	220.259
25*R*	4.0319	−18.027	20.243	5.280	−41.3458	−189.830	−415.646	218.891
25*S*	3.9899	−18.066	20.225	5.281	−45.1032	−189.949	−413.788	216.442

(*continued*)

Table 2. Continued

No	fs	hb	es	vw	FS	HB	ES	VW
26*R*	8.3509	−18.025	23.373	6.126	−37.4001	−189.903	−412.239	219.315
26*S*	8.3583	−17.982	23.357	6.122	−36.5714	−189.767	−411.100	220.576
27*R*	4.1355	−18.017	22.365	3.791	−41.9214	−186.760	−413.261	213.587
27*S*	4.1356	−18.009	22.359	3.790	−41.8770	−188.562	−414.159	216.360
28*R*	−1.1987	−18.390	20.692	5.154	−43.4428	−189.890	−415.008	217.665
28*S*	−1.1311	−18.301	20.685	5.123	−43.5873	−190.370	−415.174	220.427
29*R*	3.4975	−21.714	30.126	4.345	−35.0361	−193.174	−407.521	221.953
29*S*	3.4970	−21.713	30.125	4.345	−32.9715	−189.440	−406.044	222.422

fs, hb, es and vw: energy values of final structure, hydrogen bonding, electrostatic and van der Waals (kcal/mol) of analytes; FS, HB, ES and VW: energy values of final structure, hydrogen bonding, electrostatic and van der Waals of a complex of model phenylcarbamoylated cyclodextrin-phase and analyte; Nos. 21R–29S are calculated as a complex with TFA; unit:kcal/mol.

Table 3. Chromatographic data and molecular interaction energy values

No	ΔFS	ΔHB	ΔES	ΔVW	*k*	*α*	ΔΔFS
1	30.3745	−4.708	−6.427	18.679	3.38	1.19	3.3715
11	27.0030	−2.613	−5.011	17.551	4.01		
2	29.9789	−14.165	−8.993	25.737	0.53	1.35	0.6027
22	30.5816	−12.013	−7.698	26.698	0.72		
3*R*	36.0599	−0.375	−5.423	23.672	2.08	1.04	1.4006
3*S*	34.6593	−0.978	−5.560	23.564	2.16		
4*RR*	50.2648	−6.537	−8.029	28.573	0.19	1.62	1.8698
4*SS*	48.3950	−6.897	−7.972	27.213	0.31		
5*RR*	48.4517	−3.383	−5.906	27.265	0.17	1.00	0.4440
5*SS*	48.8957	−2.818	−5.962	27.257	0.17		
6*R*	32.7566	−1.265	−8.401	24.053	1.89*R*	1.09	0.4360
6*S*	33.1926	−4.277	−5.227	26.157	2.07*S*		
7*R*	28.8991	−8.795	−3.954	24.598	1.40	1.11	0.7805
7*S*	29.6796	−9.662	−7.320	25.003	1.56		
8*R*	36.8430	−4.193	−8.731	22.822	2.02*S*	1.35	2.4898
8*S*	34.3532	−4.710	−7.071	32.179	2.74*R*		
9*R*	32.5244	−5.487	−5.596	20.872	5.37	1.07	3.0326
9*S*	35.5570	−0.562	−1.719	28.615	5.73		
10*R*	19.8947	−8.797	−6.149	16.789	1.54	1.13	0.3207
10*S*	19.5740	−6.786	−4.497	16.991	1.36		
11*R*	30.0112	−6.108	−6.673	25.386	19.74	1.26	0.8147
11*S*	30.8259	−3.475	−4.701	26.232	24.90		
12*R*	43.1227	−3.107	−6.101	35.481	1.43	1.09	0.2904

(*continued*)

Table 3. Continued

No	ΔFS	ΔHB	ΔES	ΔVW	*k*	*α*	ΔΔFS
12*S*	42.8323	−2.819	−6.207	35.424	1.56		
13*R*	40.4985	−6.024	−7.379	32.122	1.24*S*	1.21	1.3701
13*S*	39.1284	−4.268	−9.224	31.404	1.50*R*		
14*RR*	35.2543	−10.744	−7.322	31.614	0.94	1.16	0.9285
14*SS*	37.9687	−5.038	−5.612	33.765	1.09		
15*R*	44.2703	−9.358	−6.789	35.037	0.55	1.00	0.0726
15*S*	44.1977	−13.406	−7.829	39.100	0.55		
16*R*	49.0028	−3.996	−3.527	39.298	1.18	1.17	1.0054
16*S*	50.0082	−5.929	−5.767	38.825	1.30		
17*R*	45.0306	−14.056	−8.699	37.255	0.67	1.00	0.2900
17*S*	44.7406	−5.352	−3.195	38.340	0.67		
18*R*	43.1099	−9.185	−7.108	31.745	0.62	1.00	0.0281
18*S*	43.0818	−9.199	−7.120	32.482	0.62		
19*R*	31.6953	−5.118	−5.226	30.585	2.69	1.12	1.2426
19*S*	32.9379	−8.040	−7.314	30.072	3.03		
20*R*	34.3064	−10.681	−6.874	28.578	1.73	1.05	0.6633
20*S*	33.6431	−10.920	−7.317	28.803	1.82		
21*R*	43.6758	−2.813	−6.152	24.163	0.97	1.18	1.3810
21*S*	45.0568	0.145	−8.228	25.226	0.82		

22*R*	44.3684	1.935	−1.892	28.932	0.95	1.18	2.0384
22*S*	46.4068	5.096	−3.040	26.738	0.80		
23*R*	45.0073	11.908	−4.176	21.939	0.88	1.09	2.1905
23*S*	47.1978	7.361	−2.717	25.979	0.81		
24*R*	46.5663	−0.379	−6.099	25.386	1.00	1.06	2.4928
24*S*	49.0591	3.767	−3.448	24.494	0.94		
25*R*	49.9496	7.811	−2.930	26.609	0.91	1.10	3.7154
25*S*	53.6650	7.891	−4.806	29.059	0.83		
26*R*	50.3229	7.886	−3.207	27.031	0.79	1.00	0.8213
26*S*	49.5016	7.793	−4.362	25.766	0.79		
27*R*	50.8928	4.751	−3.193	30.424	0.82	1.00	0.3083
27*S*	50.5845	6.561	−2.301	27.641	0.82		
28*R*	46.8160	7.509	−3.119	27.709	0.67	1.00	0.2121
28*S*	47.0281	8.077	−2.960	24.916	0.67		
29*R*	43.1055	7.468	−1.172	22.612	6.44	1.08	2.0651
29*S*	41.0404	3.735	−2.650	22.143	6.95		

ΔFS, ΔHB, ΔES, and ΔVW: molecular interaction energy values (kcal/mol); *k*: capacity ratio and selectivity α. Nos. 21R–29S are calculated as a complex with TFA.

For neutral compounds (solutes 1–19), for example, among the 19 compounds tested on the studied chiral stationary phase, 17 had a good correlation between $\Delta(\Delta FS)$ and α. When $\Delta(\Delta FS)$ was greater than 0.29, enantioseparation occurred ($\alpha > 1$). When $\Delta(\Delta FS)$ was less than 0.29, no separation was obtained ($\alpha = 1$). For solutes 10 and 16, the same $\Delta(\Delta FS)$ value was obtained, and while the 12th couple was separated, the 17th couple was not. Thus, the $\Delta(\Delta FS)$ limit value seems to be approximately 0.29, which was confirmed with solute 6 ($\Delta(\Delta FS) = 0.436$, $\alpha = 1.09$).

A similar conclusion was drawn for acidic compounds (solutes 21-29) that had a good correlation between $\Delta(\Delta FS)$ and α. The threshold value $\Delta(\Delta FS)$ should be in the range of 0.5 to 1.2. For this type of solute, the effect of the solvent on the calculations is very important. The obtained energy values were too high and unrealistic; even after more than 10 conformation interactions, the calculations were not believable. More comprehensive results were obtained when the effect of TFA with solute in the complex formation was taken into account. Figure 3 shows an example of an optimized structure of mandelic acid, tri-fluoro-acetic acid, and a partly locked derivatized CD complex.

Molecular mechanic calculations can be used to predict elution order. The MM calculations, however, do not provide information about the nature of the selectivity nor the absolute magnitude of the selectivity. The hydrophobic effect is a major driving force in the formation of inclusion complexes. Molecular modeling results suggest that the CD cavity is in fact highly polar and well suited for coordinating with the ammonium and carboxylic groups of amino acids.[21] This β-CD chiral stationary phase does not

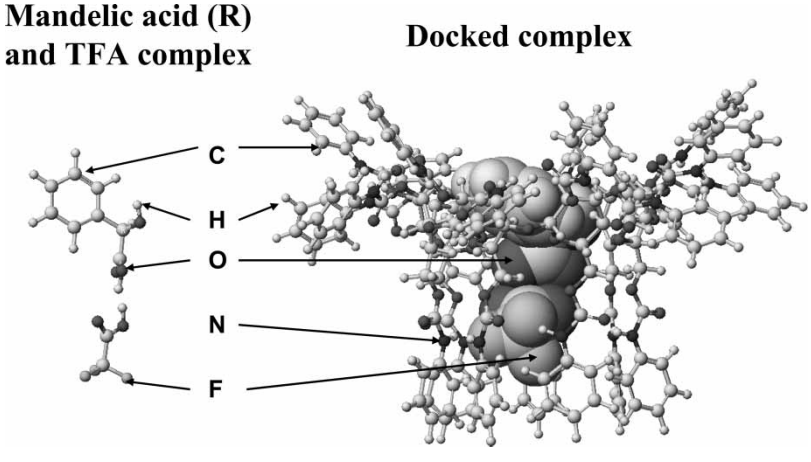

Figure 3. Optimised structure of mandelic acid, TFA, and a partly locked derivatized syclodextrin complex. Small white ball: hydrogen; gray ball: carbon; dark gray ball: nitrogen; darker gray ball: fluorine; black ball: oxygen.

appear to have a specific interaction site inside the hole, and the molecular interaction likely occurs inside the cavity. The most important function should be steric hindrance. For enantiomer separation on CD derivatives, MM calculations indicate that VW interactions are the most reliable for both association and chiral discrimination.[22–24]

The properties of CD multi-model inclusion complexes were correctly reproduced by MM2 calculations. This method allows us to correctly determine the differences in the complexation of enantiomeric forms. Special care should be taken when selecting the molecules to model and when analyzing the final geometries and interactions.[25]

CONCLUSION

In the present study, we investigated the molecular models of chiral discrimination by β-CD through differences in the interaction energies and configuration of the inclusion complexes by molecular modeling. The model β-CD derivative used in this study was not symmetrical; therefore, several dockings were adequate to obtain the optimized interaction energy values calculated using MM2 force fields of the CAChe program. The calculated results are in agreement with experimental observations for predicting the correct elution order in various enantiomer separations.

REFERENCES

1. Hanai, T. Simulation of chromatography of phenolic compounds with a computational chemical method. J. Chromatogr. A **2004**, *1027*, 279–287.
2. Hanai, T. Chromatography *in silico* for basic drugs. J. Liq. Chromatogr. & Rel. Technol. **2005**, *28* (14), 2163–2177.
3. Lipkowitz, K.B.;. Atomistic modeling of enantioselection: applications in chiral chromatography. Theor. Comp. Chem. **1998**, *5*, 329–379.
4. Hanai, T.; Hatano, H.; Nimura, N.; Kinoshita, T. Computational chemical analysis of chiral recognition in liquid chromatography, selectivity of N-(R)-1-(α-naphthyl) ethylaminocarbonyl-(R or S)-valine and N-(S)-1-(α-naphthyl)ethylaminocarbonyl-(R or S)-valine bonded aminopropyl silica gel. Anal. Chim. Acta **1996**, *332*, 213–224.
5. Hanai, T.; Hatano, H.; Nimura, N.; Kinoshita, T. Computational chemical analysis of the separation of derivatized R- and S-amino acid enantiomers on N-(tert-butylaminocarbonyl)-(S)-valylaminopropylsilica gel and (R)-1-(α-naphthyl)ethylamino carbonyl-glycylaminopropyl silica gel by liquid chromatography. J. Liq. Chromatgr. & Rel. Technol. **1996**, *19*, 1189–1204.
6. Hanai, T.; Hatano, H.; Nimura, N.; Kinoshita, T. Molecular recognition in chroma tography aided by computational chemistry. Supramol. Chem. **1994**, *3*, 243–247.

7. Lipkowitz, K.B.; Anderson, A.G. Computational aspects in supramolecular chemistry: Chiral discrimination in chromatography. NATO ASI Series, Series C: Math. Pys. Sci. **1994**, *426*, 183–198.
8. Kaliszan, R.; Noctor, T.A.G.; Wainer, I.W. Stereochemical aspects of benzodiazepine binding to human serum albumin. II. Quantitative relationships between structure and enantioselective retention in high performance liquid affinity chromatography. Mol. Pharmacol. **1992**, *42*, 512–517.
9. Daeppen, R.; Karfunkel, H.R.; Leusen, F.J.J. Computational chemistry applied to the design of chiral stationary phases for enantiomeric separation. J. Comp. Chem. **1990**, *11*, 181–193.
10. Topiol, S.; Sabio, M. Computational chemical studies of chiral stationary phase models. Complexes of methyl N-(2-naphthyl)alaninate with N-(3,5-dinitrobenzoyl)leucine n-propylamide. J. Chromatogr. **1989**, *461*, 129–137.
11. Lipkowitz, K.B.; Raghothama, S.; Yang, J.Sn. Enantioselective binding of tryptophan by α-cyclodextrin. J. Am. Chem. Soc. **1992**, *114*, 1554–1562.
12. Kano, K.; Tamiya, Y.; Otsuki, C.; Simomura, T.; Ohno, T.; Hayashida, O.; Murakami, Y. Chiral recognition by cyclic oligosaccharides. Enantioselective complexation of binaphthyl derivatives with cyclodextrins. Supramol. Chem. **1993**, *2*, 137–143.
13. Kano, K.; Kato, Y.; Kodera, M. Mechanism for chiral recognition of binaphtyl derivatives by cyclodextrins. Perkin Trans. 2: Phy. Org. Chem. **1996**, 1211–1217.
14. Murphy, R.S.; Barros, T.C.; Mayer, B.; Marconi, G.; Bohne, C.;. Photophysical and theoretical studies on the stereoselective complexation of naphthylethanols with β-cyclodextrin. Langmuir **2000**, *16*, 8780–8788.
15. Kano, K.; Hasegawa, H. Chiral recognition of helical metal complexes by modified cyclodextrins. J. Am. Chem. Soc. **2001**, *123*, 10616–10627.
16. Sun, M.; Liu, X.; Yan, L.; Luo, G.; Zhao, Y. Molecular recognition between 4a*S*/*R*-galanthamine diastereoisomers and α-cyclodextrin. J. Mol. Model. **2003**, *9*, 419–422.
17. Adeagbo, W.A.; Buss, V.; Entel, P. Chiral discrimination of 2,2′-dihydroxyl-1,1′-binaphthyl by β-cyclodextrin: a first-principles study. Phase Trans. **2005**, *78*, 677–687.
18. Fox, S.B.; Culha, M.; Sepaniak, M.J. Development of a grid search molecular mechanics modeling strategy to study elution behaviour in cyclodextrin modified capillary electrophoresis. J. Liq. Chromotogr. & Rel Technol. **2001**, *24*, 1209–1228.
19. Schaeper, J.P.; Fox, S.B.; Sepaniak, M.J. Optimization strategies and modeling of separations of dansyl-amino acids by cyclodextrin-modified capillary electrophoresis. J. Chromatogr. Sci. **2001**, *39*, 411–419.
20. Tazerouti, F.; Badjah-Hadj-Ahmed, A.Y.; Meklati, B.Y.; Pilar, F.; Minguillon, C. Enantiomeric separation of drugs and herbicides on a β-cyclodextrin/bonded stationary phase. Chirality **2002**, *14* (I), 59–66.
21. Ramirez, J.; Ahn, S.; Grigorean, G.; Lebrilla, C.B. Evidence for the formation of gas-phase inclusion complexes with cyclodextrins and amino acids. J. Am. Chem. Soc. **2000**, *122*, 6884–6890.
22. Nie, M.-Y.; Zhou, L.-M.; Wang, Q.-H.; Zhu, D.-Q. Enantiomer separation of mandelates and their analogs on cyclodextrin derivative chiral stationary phases by capillary GC. Anal. Sci. **2001**, *17*, 1183–1187.
23. Bicchi, C.; Brunelli, C.; Cravotto, G.; Rubiolo, P.; Galli, M.; Mendicuti, F. Cyclodextrin derivatives in enantiomer GC separation of volatiles. Part XXI: Complexation of some terpenoids with 2-O-acetyl-3-O-methyl- and 2-O-methyl-3-O-acetyl-

6-O-t-hexyldimethylsilyl-γ-cyclodextrins: Molecular mechanics and molecular dynamics. J. Sep. Sci. **2003**, *26*, 1479–1490.
24. Wensheng, C.; Yanmin, Y.; Xueguang, S. Chiral recognition of aromatic compounds by β-cyclodextrin based on bimoldal complexation. J. Mol. Model. **2005**, 10.1007/s00894-004-0233-6.
25. Perez, F.; Jaime, C.; Sanchez-Ruiz, X. MM2 calculations on cyclodextrins: Multimodal inclusion complexes. J. Org. Chem. **1995**, *60*, 3840–3845.

Received June 22, 2007
Accepted July 11, 2007
Manuscript 6145